

*ARMY RESEARCH LABORATORY*



## **Patterning of Bi<sub>2</sub>Te<sub>3</sub> Polycrystalline Thin-Films on Silicon**

**by Brian Morgan and Patrick Taylor**

---

**ARL-TR-4351**

**January 2008**

## **NOTICES**

### **Disclaimers**

The findings in this report are not to be construed as an official Department of the Army position unless so designated by other authorized documents.

Citation of manufacturer's or trade names does not constitute an official endorsement or approval of the use thereof.

# **Army Research Laboratory**

Adelphi, MD 20783-1197

---

---

**ARL-TR-4351**

**January 2008**

---

## **Patterning of Bi<sub>2</sub>Te<sub>3</sub> Polycrystalline Thin-Films on Silicon**

**Brian Morgan and Patrick Taylor**  
Sensors and Electron Devices Directorate, ARL

# REPORT DOCUMENTATION PAGE

*Form Approved*  
*OMB No. 0704-0188*

Public reporting burden for this collection of information is estimated to average 1 hour per response, including the time for reviewing instructions, searching existing data sources, gathering and maintaining the data needed, and completing and reviewing the collection information. Send comments regarding this burden estimate or any other aspect of this collection of information, including suggestions for reducing the burden, to Department of Defense, Washington Headquarters Services, Directorate for Information Operations and Reports (0704-0188), 1215 Jefferson Davis Highway, Suite 1204, Arlington, VA 22202-4302. Respondents should be aware that notwithstanding any other provision of law, no person shall be subject to any penalty for failing to comply with a collection of information if it does not display a currently valid OMB control number.

**PLEASE DO NOT RETURN YOUR FORM TO THE ABOVE ADDRESS.**

<b>1. REPORT DATE (DD-MM-YYYY)</b> January 2008		<b>2. REPORT TYPE</b> Final		<b>3. DATES COVERED (From - To)</b>	
<b>4. TITLE AND SUBTITLE</b> Patterning of Bi2Te3 Polycrystalline Thin-Films on Silicon				<b>5a. CONTRACT NUMBER</b>	
				<b>5b. GRANT NUMBER</b>	
				<b>5c. PROGRAM ELEMENT NUMBER</b>	
<b>6. AUTHOR(S)</b> Brian Morgan and Patrick Taylor				<b>5d. PROJECT NUMBER</b>	
				<b>5e. TASK NUMBER</b>	
				<b>5f. WORK UNIT NUMBER</b>	
<b>7. PERFORMING ORGANIZATION NAME(S) AND ADDRESS(ES)</b> U.S. Army Research Laboratory ATTN: AMSRD-ARL-SE-DP 2800 Powder Mill Road Adelphi, MD 20783-1197				<b>8. PERFORMING ORGANIZATION REPORT NUMBER</b>  ARL-TR-4351	
<b>9. SPONSORING/MONITORING AGENCY NAME(S) AND ADDRESS(ES)</b>				<b>10. SPONSOR/MONITOR'S ACRONYM(S)</b>	
				<b>11. SPONSOR/MONITOR'S REPORT NUMBER(S)</b>	
<b>12. DISTRIBUTION/AVAILABILITY STATEMENT</b> Approved for public release; distribution is unlimited.					
<b>13. SUPPLEMENTARY NOTES</b>					
<b>14. ABSTRACT</b> Bi2Te3-based thermoelectric (TE) energy conversion devices are an attractive possibility for recovering usable energy from waste heat. The integration of TE devices on silicon substrates opens the door for new highly integrated systems where micro-electro-mechanical systems (MEMS) heat exchangers and sensor/actuator technology can be leveraged to improve conversion efficiency and system capability. One roadblock on this path is the development of reliable patterning methods for fabricating thin-film TE devices on silicon micromachined substrates. This report gives the results from investigating patterning techniques for polycrystalline Bi2Te3 films grown using molecular beam epitaxy (MBE). Lithographic patterning and both wet and dry etch techniques are discussed. Results show that the developed processes can be used to precisely pattern features smaller than 10 μm on a side and are scalable to vertical dimensions (>> or ≥) 10 μm.					
<b>15. SUBJECT TERMS</b> Radar signature, computational electromagnetics					
<b>16. SECURITY CLASSIFICATION OF:</b>			<b>17. LIMITATION OF ABSTRACT</b>  SAR	<b>18. NUMBER OF PAGES</b>  18	<b>19a. NAME OF RESPONSIBLE PERSON</b> Brian Morgan
<b>a. REPORT</b> U	<b>b. ABSTRACT</b> U	<b>c. THIS PAGE</b> U			<b>19b. TELEPHONE NUMBER (Include area code)</b> (301) 394-0926

---

## Contents

---

<b>List of Figures</b>	<b>iv</b>
<b>List of Tables</b>	<b>iv</b>
<b>1. Introduction</b>	<b>1</b>
<b>2. Sample Preparation</b>	<b>2</b>
<b>3. Photolithography</b>	<b>4</b>
<b>4. Wet Chemical Etching</b>	<b>5</b>
<b>5. Dry Plasma Etching</b>	<b>6</b>
<b>6. Conclusion</b>	<b>9</b>
<b>References</b>	<b>10</b>
<b>Acronyms</b>	<b>11</b>
<b>Distribution List</b>	<b>12</b>

---

## List of Figures

---

Figure 1. Conceptual schematic of a TE generator on silicon, where heat exchangers can be micromachined in silicon and integrated with MEMS sensors/actuators onto a single chip.....	2
Figure 2. Figure of merit ( $Z$ ) as a function of temperature for a variety of materials; for room temperature applications, $\text{Bi}_2\text{Te}_3$ -based compounds are the obvious choice (2).....	3
Figure 3. Optical micrograph of a $\text{Bi}_2\text{Te}_3$ sample after lithography—the patterned photoresist squares are nicely defined; however, the development step has caused significant delamination of $\text{Bi}_2\text{Te}_3$ where metal is not present to anchor it down.....	4
Figure 4. SEMs of wet etched $\text{Bi}_2\text{Te}_3$ , showing (a) the large horizontal mask undercut and resulting residue that is quite evident and (b) a close-up of the resulting vertical sidewall .....	6
Figure 5. SEMs of etched $\text{Bi}_2\text{Te}_3$ posts on pre-patterned metal pads—note lack of residue on metal as well as the verticality of the sidewalls.....	8

---

## List of Tables

---

Table 1. Measured etch rate ( $\mu\text{m}/\text{min}$ ) as a function of chamber pressure and gas mixture (all at 100 W electrode power).....	7
Table 2. Measured etch rates and selectivity to photoresist (PR) as a function of chamber pressure and electrode power (all using 15/5/15sccm of $\text{CH}_4/\text{H}_2/\text{Ar}$ ).....	7
Table 3. Initial and final etch recipe parameters.....	8

---

## 1. Introduction

---

Waste heat conversion is an area of significant interest to the Army, as >50% of the input energy to an internal combustion engine can be lost as heat. Should a fraction of this energy be recovered, significant benefits in power output and system efficiency could be realized. In their usual form, thermoelectric (TE) devices are fabricated from “bulk” materials that are synthesized by freezing molten boules forming ingots. Those ingots proceed through serial processes including saw-cut dicing, metallization, and soldering on the path towards a TE device. While bulk device fabrication is well-known and mature, miniaturizing that process for micromachined TE devices for small and/or complex systems becomes difficult given their limited size and serial manufacturing techniques. In contrast, micromachined TE generators could take advantage of the huge infrastructure that exists for parallel manufacturing of silicon-based microsystems to improve device yield, system performance, integration, and form factor. Applications such as unattended ground sensors, thermal imagers, or clandestine tagging, tracking, and locating (cTTL) are just some of the possible areas where this technology could be beneficial.

Industry demonstrations of thin-film TE devices include output powers of >14 W from a 4.6 cm<sup>2</sup> device at  $\Delta T \sim 100$  °C, with reported efficiencies of 5–10% (*1*). However, TE materials are typically grown on expensive, exotic substrates like barium fluoride (BaF) or gallium arsenide (GaAs), neither of which is scalable compared to silicon, nor do they offer the ability to integrate electronic devices and/or sensors as silicon does. Thus, the goal of this research is to combine three areas of active research within the Microsystem thrust of the U.S. Army Research Laboratory (ARL) (TE materials, micro-electro-mechanical systems (MEMS) sensors/actuators, and thermal management) into a single-chip system similar to that shown conceptually in figure 1. This report details the technical progress and limitations of directly patterning TE thin-films on silicon for improved form factor, reduced system complexity, and superior thermal interfaces.

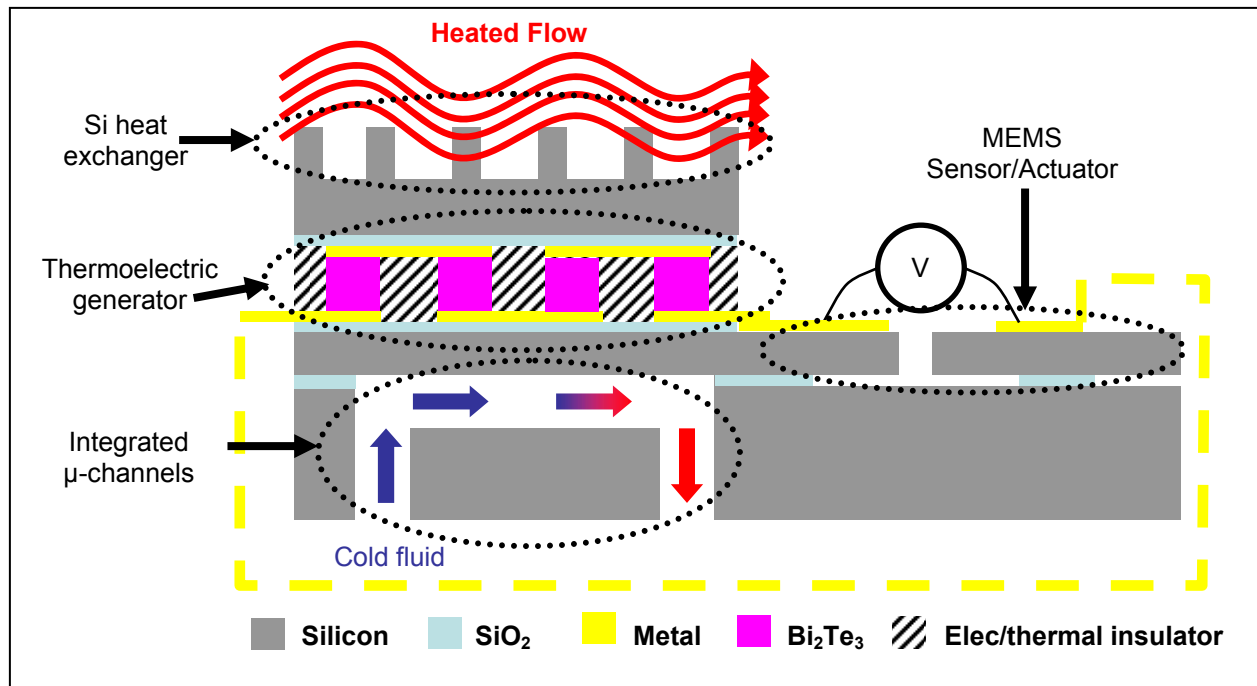


Figure 1. Conceptual schematic of a TE generator on silicon, where heat exchangers can be micromachined in silicon and integrated with MEMS sensors/actuators onto a single chip.

## 2. Sample Preparation

In general, when selecting a material for a TE device, one desires three characteristics: (1) high electrical conductivity to minimize electrical resistance losses, (2) low thermal conductivity to maximize the temperature gradient across the material, and (3) a high Seebeck coefficient to maximize the thermal voltage. These properties are typically expressed as the so-called “figure of merit ( $Z$ )” (2):

$$Z = \frac{\alpha^2 \cdot \sigma}{\kappa} \quad (1)$$

where  $\alpha$  is the Seebeck coefficient (V/K),  $\sigma$  is electrical conductivity ( $\Omega^{-1}\text{m}^{-1}$ ), and  $\kappa$  is thermal conductivity ( $\text{Wm}^{-1}\text{K}^{-1}$ ). The figure of merit is plotted as a function of temperature in figure 2 (2). Given that many energy scavenging applications are in the near-room temperature regime (0–150 °C), bismuth telluride ( $\text{Bi}_2\text{Te}_3$ )-based materials offer the highest potential performance. Other efforts on lead-telluride ( $\text{PbTe}$ )-based materials for higher temperature applications are being pursued through a collaboration with the University of Florida (3).

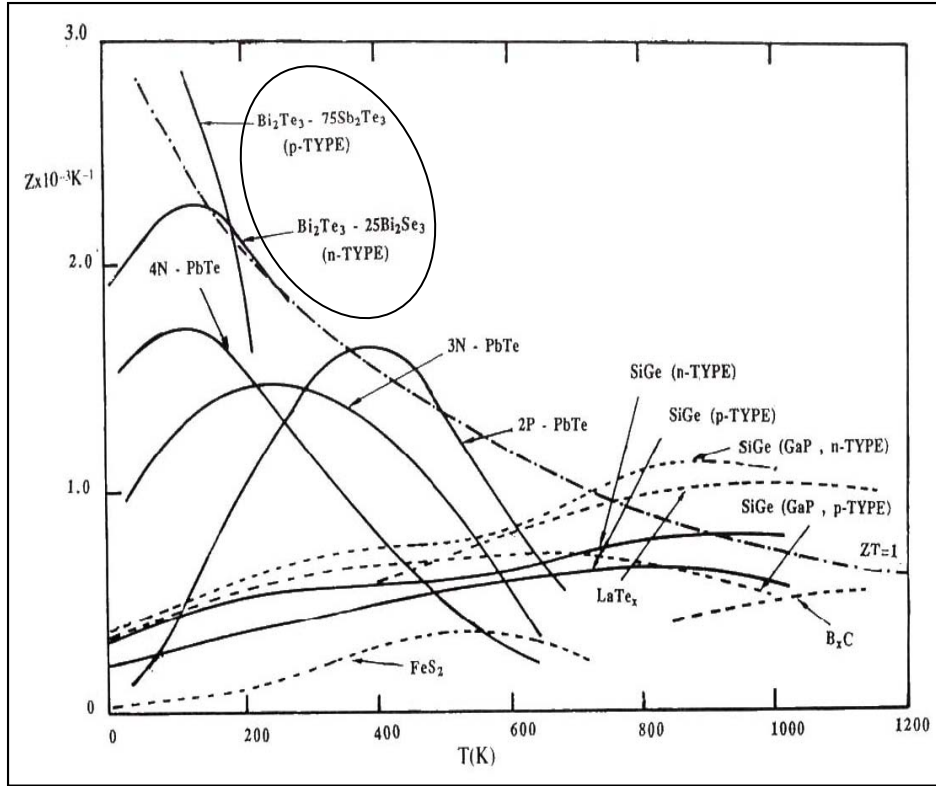


Figure 2. Figure of merit ( $Z$ ) as a function of temperature for a variety of materials; for room temperature applications,  $\text{Bi}_2\text{Te}_3$ -based compounds are the obvious choice (2).

The samples used in this research started as 4-in  $\langle 100 \rangle$  silicon wafers. A  $1 \mu\text{m}$  thermal oxide was grown over the entire wafer to electrically insulate the TE device material from the silicon. Various metal pads were then defined using a standard lithography process (AZ5214) and lift-off in acetone ( $50^\circ\text{C}$  for 2 h). These patterned metal pads will eventually form bottom side interconnects between TE posts. After substrate cleaning in an RCA-1 bath to remove organic residue, the blanket  $\text{Bi}_2\text{Te}_3$  films were grown using solid-source molecular beam epitaxy (MBE). As deposited, the films were undoped, and growth rates of  $\sim 1 \mu\text{m}/\text{h}$  were demonstrated. Thus far, films as thick as  $9 \mu\text{m}$  have been achieved (reactor time limited), although there appears to be no upper limit to the thickness and thicker films are planned for future devices. After film growth, the sample is coated with a thin photoresist layer to protect the  $\text{Bi}_2\text{Te}_3$  during a dicing step, in which 15 by 15 mm dies are separated for processing. The protective photoresist layer is removed in a PRS-3000 photoresist stripper for 2 min at  $80^\circ\text{C}$ .

---

### 3. Photolithography

---

Before etching experiments could be undertaken, a photolithography step was used to create the appropriate pattern. Standard lithography recipes were adapted for this purpose. The best results were obtained using the following sequence: (1) spin coat AZ5214e at 1200 rpm for 30 s, (2) soft bake at 110 °C for 60 s, (3) contact exposure for 3.3 s, (4) reverse-image bake at 120 °C for 30 s, (5) flood exposure for 5.5 s, and (6) develop for 60 s in AZ312MIF 1:1 DI. This resulted in a 2.8 μm thick photoresist layer in which features as small as 4 μm square were consistently defined. In general, the exposure times were the only parameters requiring significant attention, a fact largely attributed to the reduced reflectivity and increased light absorption of the polycrystalline Bi<sub>2</sub>Te<sub>3</sub> surface compared to polished single crystal silicon.

The primary problem encountered during lithography was delamination during the development step. As shown in figure 3, on/around areas with pre-patterned metal pads, the Bi<sub>2</sub>Te<sub>3</sub> adhered, while in open areas with only bare SiO<sub>2</sub> the film delaminated, likely from the lack of any chemical bonding to the surface. While figure 3 is an extreme case, such delamination is of little concern since most implementations will require metal underneath the Bi<sub>2</sub>Te<sub>3</sub> post to serve as an electrical interconnect. In the future, the ability to grow single crystal Bi<sub>2</sub>Te<sub>3</sub> directly on single crystal silicon may be investigated as an alternative means for improving film adhesion and doping at the expense of slightly more complicated system design.

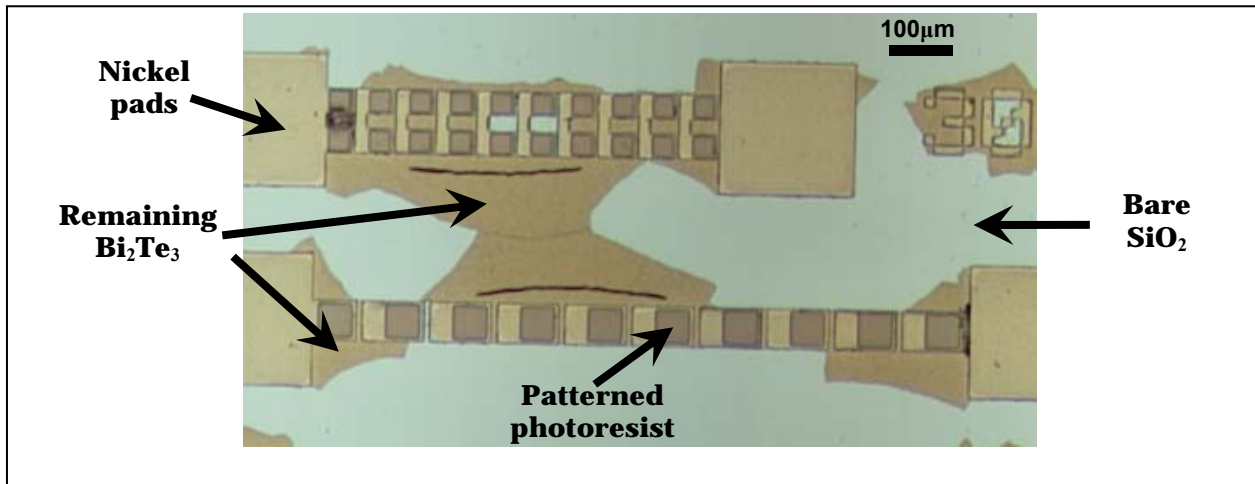


Figure 3. Optical micrograph of a Bi<sub>2</sub>Te<sub>3</sub> sample after lithography—the patterned photoresist squares are nicely defined; however, the development step has caused significant delamination of Bi<sub>2</sub>Te<sub>3</sub> where metal is not present to anchor it down.

---

## 4. Wet Chemical Etching

---

Wet chemical etching was first pursued due to its simplicity and availability. According to Dilberto et al. (4), a combination of hydrogen peroxide ( $\text{H}_2\text{O}_2$ ), hydrochloric acid (HCl), and de-ionized water (DI) has proven effective at etching  $\text{Bi}_2\text{Te}_3$ -based compounds. However, particular attention should be given to the compatibility of wet chemical etchants with other materials on the wafer. In this case, the  $\text{H}_2\text{O}_2$ :HCl:DI mix is essentially a diluted form of the standard RCA-2 clean, which would etch both the  $\text{Bi}_2\text{Te}_3$  device material as well as the metal pad. As an alternative, Shafai and Brett (5) used a diluted combination of HCl and nitric acid ( $\text{HNO}_3$ ), a variant of the common “Aqua Regia.” Since we desire to use photoresist as the masking material for process flexibility, we used a diluted version of Aqua Regia (3 HCl:1  $\text{HNO}_3$ :2 DI) that according to Williams et al. (6) should not attack photoresist appreciably.

Vertical etch rates of  $\sim 0.5\mu\text{m}/\text{min}$  were achieved; however, the scanning electron microscope (SEM) images shown in figure 4 highlight that the horizontal undercut is  $>5$  times the thickness. This fact indicates that there may be more exposed surface area in contact with the etchant because of, say, grain boundary effects and open voids within the material that causes the relatively fast lateral etch rate. While the grain structure and the presence of voids within the material can be improved in future growth studies, the best scenario for wet etching a polycrystalline material is still a 1:1 ratio of vertical to horizontal etch rates. Figure 4(a) also shows some residue that remained after the wet etch was performed. Energy-dispersive x-ray spectroscopy (EDX) analysis indicates this to be a carbon-based residue (7), likely from partial etching of the photoresist during immersion in the solution. Further dilution of the etchants could mitigate this effect (at the cost of etch rate), or the migration to a metal mask could be investigated.

Thus, while the wet approach offers reasonable etch rates ( $>0.5\mu\text{m}/\text{min}$ ) and requires very simple bench-top equipment, wet patterning must be limited to low aspect ratio structures. Since TE generators perform most efficiently at high aspect ratios, an alternative technique is necessary to pattern smaller features.

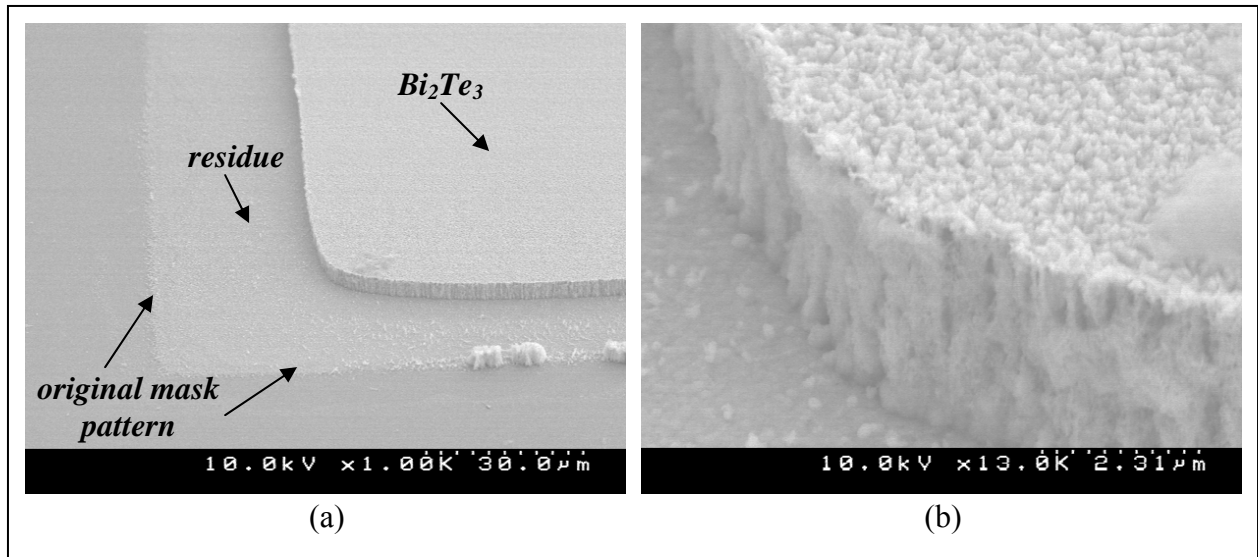


Figure 4. SEMs of wet etched  $\text{Bi}_2\text{Te}_3$ , showing (a) the large horizontal mask undercut and resulting residue that is quite evident and (b) a close-up of the resulting vertical sidewall.

## 5. Dry Plasma Etching

Dry plasma etching should provide the desired vertical etch characteristics; however, achieving significant etch rates and good selectivity to a photoresist mask is typically challenging. In addition, the capital equipment required is both complicated and expensive. For this work, we used an inductively coupled plasma (ICP) etch tool that allows independent tuning of the plasma density and ion energy. Literature reports show some success using common etch gasses (such as Ar,  $\text{O}_2$ ,  $\text{CH}_4$ , etc.) with etch rates of  $\sim 60$  nm/min (4). Combinations of  $\text{CH}_4$ - $\text{H}_2$  are often used for etching III-V devices in the same ICP chamber, and were therefore considered a good starting point. Each 15 by 15 mm die was mounted on bare 4-in silicon carrier wafers for handling by the system.

Using established recipes as a guideline, the initial experiments were focused on understanding the basic dependence of the  $\text{Bi}_2\text{Te}_3$  etch rates in different gas mixtures and pressures. For the gas mixture, an initial combination of 10 sccm of  $\text{CH}_4$ ,  $\text{H}_2$ , and Ar was compared to 15 sccm  $\text{CH}_4$ , 5 sccm  $\text{H}_2$ , and 15 sccm of Ar. In the latter mixture, it was expected that the increase in heavy  $\text{Ar}^+$  molecules bombarding the surface would promote ion-assisted etching, while an increase in  $\text{CH}_x$  radicals would increase chemical etching, leading to a dramatic increase in etch rate. The two pressure set-points were intended to investigate the tradeoffs between available etch species, average ion energy, and possible re-deposition of volatiles, all of which are known to affect the etch rate.

As shown in table 1, the initial recipe resulted in an etch rate of 0.22  $\mu\text{m}/\text{min}$ , while changing the pressure and gas mixture successfully increased the etch rate to 0.66  $\mu\text{m}/\text{min}$ , with pressure change having a greater influence than chemistry. This relatively high etch rate is important, because it represents a tenfold improvement over that reported in Dilberto et al. (4) and makes etching thick films ( $>10 \mu\text{m}$ ) possible in realistic time. However, during this etch, we observed a selectivity of  $<5:1$ , meaning that the photoresist mask thickness must increase dramatically to etch thicker films, which in turn will reduce the resolution achievable in the resist. Therefore, a second round of experiments was devised to investigate improving the selectivity—a notoriously difficult property to control given that, for example, a change in ion energy effects the etch rates of both the  $\text{Bi}_2\text{Te}_3$  and photoresist. We chose to vary the electrode power and pressure in an attempt to minimize ion bombardment on the photoresist while maintaining enough ion assisted etching of the  $\text{Bi}_2\text{Te}_3$  to realize a significant overall etch rate. The gas combination of 15/5/15 was employed for all cases and the results are shown in table 2. For the case of higher electrode power (100 W), the low pressure had a slightly higher selectivity, but a vastly lower etch rate. For the lower electrode power (50 W), the etch rate decreased only slightly while the selectivity effectively doubled. Thus, a final etch rate  $>0.5 \mu\text{m}/\text{min}$  with selectivity well above 10:1 was achieved through simple changes in gas mixture, electrode power, and pressure. The initial and final etch parameters are shown in table 3.

Table 1. Measured etch rate ( $\mu\text{m}/\text{min}$ ) as a function of chamber pressure and gas mixture (all at 100 W electrode power).

Gas Mix $\text{CH}_4/\text{H}_2/\text{Ar}$ (sccm)	Pressure (mTorr)	
	10	20
10/10/10	0.22	0.47
15/5/15	0.28	0.66

Table 2. Measured etch rates and selectivity to photoresist (PR) as a function of chamber pressure and electrode power (all using 15/5/15sccm of  $\text{CH}_4/\text{H}_2/\text{Ar}$ ).

Etch Rate ( $\mu\text{m}/\text{min}$ ) / Selectivity ( $\text{Bi}_2\text{Te}_3:\text{PR}$ )		Pressure (mTorr)	
		10	20
Electrode Power (W)	50	0.24 / 12.1	0.56 / 14.7
	100	0.28 / 6.5	0.66 / 5.0

Table 3. Initial and final etch recipe parameters.

	Coil Power (W)	Electrode Power (W)	Chamber Pressure (mTorr)	Gas Flow (sccm)		
				CH <sub>4</sub>	H <sub>2</sub>	Ar
<b>Initial</b>	600	100	10	10	10	10
<b>Final</b>	600	50	20	15	5	15

SEM images of prototype TE posts on patterned metal features are shown in figure 5. Note the lack of residue and vertical sidewall profiles achieved, establishing this etching technique as a viable tool for fabricating micromachined TE legs. The developed techniques should enable scaling of similar structures to even thicker films, enabling improved performance of waste heat recovery systems.

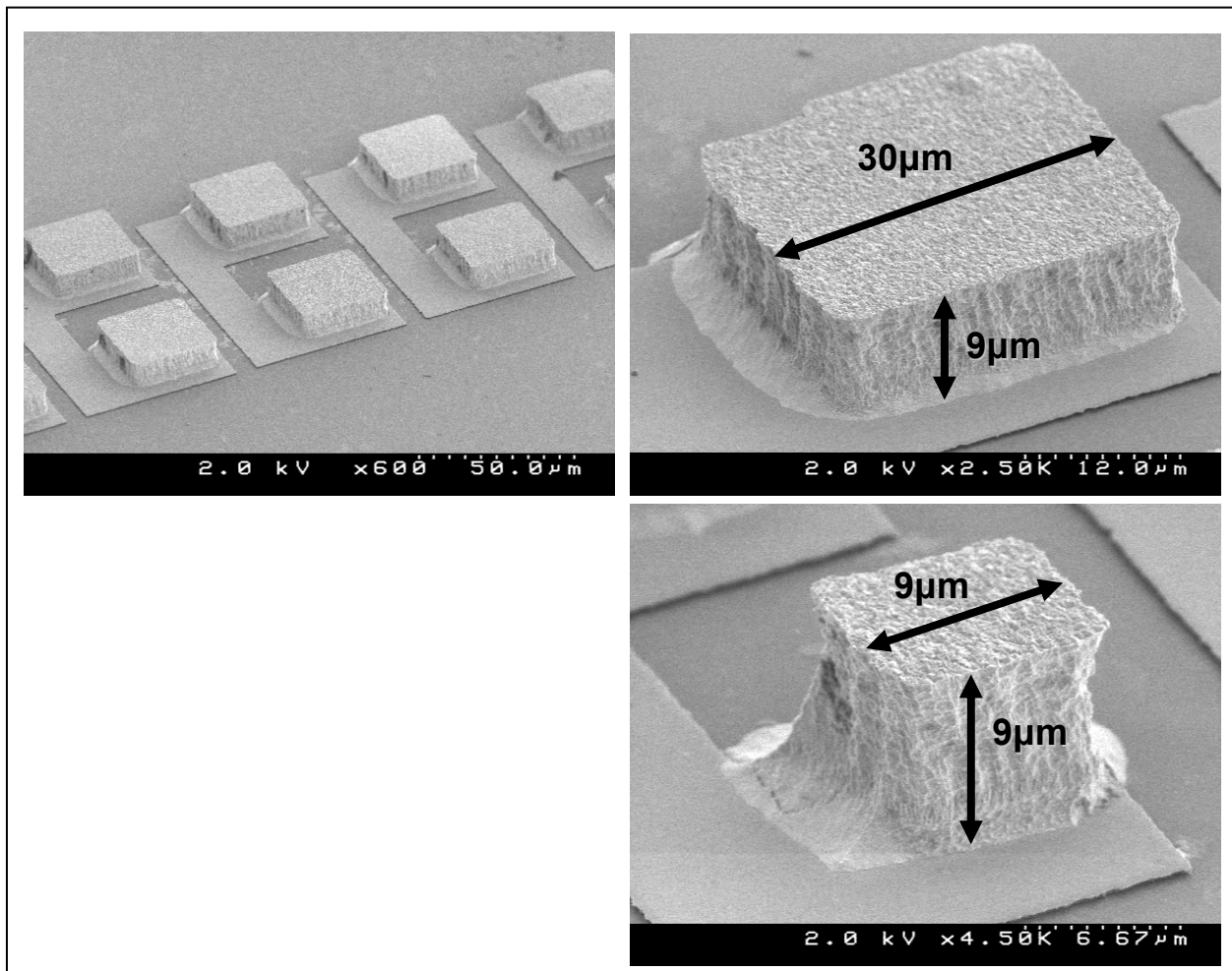


Figure 5. SEMs of etched Bi<sub>2</sub>Te<sub>3</sub> posts on pre-patterned metal pads—note lack of residue on metal as well as the verticality of the sidewalls.

---

## 6. Conclusion

---

This research has demonstrated that Bi<sub>2</sub>Te<sub>3</sub>-based TE materials and devices can be monolithically integrated with silicon-based materials and MEMS most efficiently provided there is an “adherent” on the SiO<sub>2</sub> surface. For this work, a base metal is highly successful and necessary for eventual device fabrication anyway. These Bi<sub>2</sub>Te<sub>3</sub> TE thin-films can be reliably patterned using the existing, large technology infrastructure available within silicon processing facilities. Experiments have shown that high etch rates (>0.5 μm/min) and photoresist selectivity (>10:1) can be achieved through straight-forward process modifications. Future work will concentrate on using these fabrication techniques to create characterization structures in order to measure and optimize the TE properties of these films.

---

## References

---

1. Venkatasubramanian, R. et al. Microscale thermoelectric devices for energy harvesting and thermal management. *Proceedings of Power MEMS 2006*, Berkeley, CA, 2006, pp 1–4.
2. Rowe, D. M. *CRC Handbook of Thermoelectrics*, CRC Press: Boca Raton, FL, 1995.
3. Boniche, I. et al. Progress towards a micromachined thermoelectric generator using PbTe and PbSnSeTe thin films. *Proceedings of Power MEMS 2006*, Berkeley, CA, 2006, pp195–199.
4. Dilberto, S. et al. A technology for a device prototyping based on electrodeposited thermoelectric V-VI layers. *22<sup>nd</sup> International Conference on Thermoelectrics*, 2003, pp 661–664.
5. Shafai, C.; Brett, M. J. A Micro-Integrated Peltier Heat Pump for Localized On-Chip Temperature Control, *Canadian Conference on Electrical and Computer Engineering*, 26–29 May 1996, 88–91.
6. Williams, K. et al. Etch Rates for Micromachining Processing – Part II. *J. of Microelectromechanical Systems* **December 2003**, 12, (6), 761–777.
7. Taylor, P. J.; Lee, U.; Morgan, B.; Dhar, N. K. *Analysis of Residues Resulting From Etching Micro-scale Thermoelectric MEMS*; ARL-TR-4135; U.S. Army Research Laboratory: Adelphi MD, May 2007.

---

## Acronyms

---

ARL	U.S. Army Research Laboratory
BaF	barium fluoride
Bi <sub>2</sub> Te <sub>3</sub>	bismuth telluride
cTTL	clandestine tagging, tracking, and locating
DI	de-ionized
EDX	energy-dispersive x-ray spectroscopy
GaAs	gallium arsenide
H <sub>2</sub> O <sub>2</sub>	hydrogen peroxide
HCl	hydrochloric acid
HNO <sub>3</sub>	nitric acid
ICP	inductively coupled plasma
MBE	molecular beam epitaxy
MEMS	micro-electro-mechanical systems
PbTe	lead-telluride
SEM	scanning electron microscope
TE	thermoelectric

---

## Distribution List

---

<u>No. of</u> <u>Copies</u>	<u>Organization</u>	<u>No. of</u> <u>Copies</u>	<u>Organization</u>
1 elec	ADMNSTR DEFNS TECHL INFO CTR DTIC OCP (ELECTRONIC COPY) 8725 JOHN J KINGMAN RD STE 0944 FT BELVOIR VA 22060-6218	1 HC	US ARMY RESEARCH LAB AMSRD ARL SE RL P AMIRATHRAJ 2800 POWDER MILL ROAD ADELPHI MD 20783-1197
5 CDs	US ARMY RSRCH LAB IMNE ALC IMS MAIL & RECORDS MGMT AMSRD ARL D J M MILLER AMSRD ARL CI OK TL TECHL LIB AMSRD ARL CI OK T TECHL PUB (2 copies) 2800 POWDER MILL ROAD ADELPHI MD 20783-1197	1 HC	US ARMY RESEARCH LAB AMSRD ARL SE E G WOOD 2800 POWDER MILL ROAD ADELPHI MD 20783-1197
1 CD	US ARMY RESEARCH LAB AMSRD CI OK TP TECHL LIB ATTN T LANDFRIED APG MD 21005	1 HC	CERDEC – C2D ARMY POWER DIV CHIEF ENGINEER AMSRD CER C2 AP ES C BOLTON 10125 GRATOIT RD STE 100 FT BELVOR VA 22060
5 HCs	US ARMY RESEARCH LAB AMSRD ARL SE DP B MORGAN B GEIL C M WAITS N JANKOWSKI J HOPKINS 2800 POWDER MILL ROAD ADELPHI MD 20783-1197	1 HC	DARPA DSO S BEERMAN-CURTIN 3701 NORTH FAIRFAX DRIVE ARLINGTON VA 22203-1714
		22	(1 elec, 6 CDs, 15 HCs)
5 HC	US ARMY RESEARCH LAB AMSRD ARL SE EI P TAYLOR N DHAR F SEMENDY M DUBEY H POLLEHN 2800 POWDER MILL ROAD ADELPHI MD 20783-1197		
1 HC	US ARMY RESEARCH LAB AMSRD ARL SE E D E SHAFFER 2800 POWDER MILL ROAD ADELPHI MD 20783-1197		